The Development and Testing of a Lab-Scale Tidal Stream Turbine for the Study of Dynamic Device Loading

Matthew Allmark*‡, Robert Ellis*§, Kate Porter†¶, Tim O'Doherty*‖, and Cameron Johnstone†**
*School of Engineering
Cardiff University,The Parade Cardiff, Wales. CF24 3AA

†Department of Mechanical and Aerospace Engineering
University of Strathclyde, James Weir Building, Level 8, 75 Montrose Street, Glasgow, G1 1XJ

‡Allmarkmj1@cardiff.ac.uk
§ellisR10@cardiff.ac.uk
¶kate.johannesen@strath.ac.uk
‖odoherty@cardiff.ac.uk
**cameron.johnstone@strath.ac.uk

***Abstract*—The paper outlines the development and testing of a 0.9 m diameter lab-scale Horizontal Axis Tidal Turbine. The turbine was developed based on design experience acquired at Cardiff University during the development and testing of a number of legacy lab-scale Horizontal Axis Tidal Turbines. The development process was also considerate of design activities undertaken elsewhere within research. The development of the aforementioned Horizontal Axis Tidal Turbines was undertaken specifically to test under dynamic lab-scale conditions including both wave, turbulence and, ultimately, dynamic loadings caused by array interaction effects.**

***Index Terms*—Model Turbine Development, Scale HATT, Dynamic Loading of HATTs.**

I. Introduction

Energy extraction from the ocean's tides has gained widespread acceptance as a potential contributor to the UK energy mix [1]. Increased interest in tidal energy extraction has, in part, been driven by the realisation of finite global resources and environmental impacts of burning fossil fuels [2]. The EU Renewable Energy Directive outlines ambitions of the EU community to fulfil 20% of its energy needs via renewable sources by 2020; it is foreseen that tidal energy extraction could go some way to helping achieve this target [1].

In order for Horizontal Axis Tidal Turbine (HATT) devices to generate energy at a competitive levelized cost of energy (LCOE), effective strategies for reducing device over-engineering and the burden of operation and maintenance costs are required. In order to achieve the 20 year lifespan [3] - quoted as being required for cost effective energy extraction - whilst reducing device over engineering, detailed understanding of HATT operational loads is required. Knowledge of normal operational loads, extreme operational loads and the characteristics of load fluctuations is required to minimise the probability of device failure due to overloading and fatigue.

During the projected turbine life cycle, extreme loads can arise from current-wave interactions, from flow acceleration around upstream turbines and from high speed turbulent structures in the on-coming fluid flow. Furthermore, these loads sources, as well as the effects of tidal cycles and turbine rotation, lead to a variety of cyclic loading events at various magnitudes and frequencies. In moving towards robust and cost effective designs, understanding and quantification of these loads will be required. It would seem pertinent to develop a series of standard load specifications under a number of operational and environmental scenarios to which turbines can be designed and ultimately 'signed-off' against - similar to the IEC 61400 standard for the wind industry [4]. Although difficulties in adapting such an approach to the tidal industrial surely exist, such a methodology will allow for increased load understanding, design maturity and improved turbine life expectancy forecasting. Developments in the above are likely bolster investor confidence and will aid in device underwriting by insurance companies - two important aspects that need to be addressed in order to create a functioning industry for the future.

As a brief illustration of the difficulties faced by the industry going forward, and to give context to the complexities inherent in turbine load quantification, one may consider that a HATT operating in a reasonably standard wave-current climate - average wave period of 2 s [5] - may be subjected to potentially $2 * 10^8$ load cycles due to wave loading. A HATT of 20 m diameter subjected to average flow velocities may experience up to $0.6 * 10^8$ gravitation, shear profile, buoyancy and tower shadowing load fluctuations associated with turbine rotation. Lastly, due to the interaction between various flow aspects it is

not yet clear that the effects of fatigue loads are as significant as HATT overloading, as had been established in the wind industry [6].

In order to drive understanding of the loading sources outlined in the previous section, a research project known as Dynamic Loading of Tidal Turbine Arrays or DyLoTTA is currently being undertaken. The project is a joint project between the Cardiff Marine Energy Research Group (CMERG) based at Cardiff University and the Department of Mechanical and Aerospace Engineering at the University of Strathclyde. The work seeks to develop more detailed understanding of dynamic turbine load cases through a combination of 1/20th scale testing, Blade Element Momentum Theory (BEMT) Modelling, Computational Fluid Dynamics Modelling and Finite Element Modelling. Here the goal is to present findings and datasets relating to HATT operation under various wave-current and turbulence scenarios as both individual devices and as turbine Arrays. Furthermore, the project seeks to quantify the effects of turbine control, management and monitoring approaches on loading parameters, turbine life expectancy and ultimately LCOE.

This paper outlines the development process undertaken in generating a design for an instrumented 1/20th scale HATT device. Ultimately, three of the outlined HATTs will be created and used for testing of HATTs singularly and in array configurations. The paper continues with a review of lab-scale turbines developed to date, the next section outlines the design and design considerations of the overall turbine and specific aspects of the turbine. In the preceding section the process of initial characterisation of the 1/20th scale HATT at the INSEAN Wave Tow Tank facility in Rome is presented. The paper closes with a brief discussion and conclusions.

II. Literature Review

The CMERG has previously developed two working 0.5m meter diameter flume based turbines. These have been used to conduct turbine design studies using CFD. Both of the turbines were developed using the horizontal axis tidal turbine (HATT) form. Details of the first turbine setup can be found in [7]. This turbine consisted of a rotor submerged in a re-circulating flume tank. The rotor could be coupled via either a flexible or rigid drive shaft to a 1.28 KW Baldor brushless AC servomotor, which was situated above the flume. The Baldor motor was used to supply a braking torque to the rotor to provide control over the turbines rotational velocity for a given flow rate. The regeneration energy produced was dumped into a 1 K resistor and dissipated as heat. Testing with the first generation turbine was successful in validating and informing CFD models developed within the research group.

During this early work on turbine characterisation and model validation a BEMT model was used to test the given blade design for optimum pitch angle of the blade tip measured relative to the rotational plane of the turbine [7](Mason-Jones, 2010). The optimum pitch angle for the blade profile used was found to be 6^o. The previously proven blade design was used in the 2nd generation turbine model. This allowed the same blade sets to be used on each turbine, minimising the relatively high cost of blade manufacture; each of the 21 blades manufactured cost approximately 1 000. Further details of the second-generation turbine are outlined in [8] [9]. It was developed by mounting the braking motor directly behind the turbine rotor. The turbine rotor and braking motor were directly coupled via a short drive shaft. This required that the motor was mounted inside the turbine housing, i.e. in the manner that is similar to many commercial turbine set ups with the motor taking the position of a permanent magnet synchronous generator (typically used for direct drive applications). Thrust on the turbine structure, including the stanchion, was measured via a 50 Kg force block mounted at the connection between the turbine stanchion and the cross-beam holding the stanchion. This turbine was used extensively in studying the power converted and wake recovery associated with the rotor under plug flows, profiled flows, and under wave current interaction scenarios [10] [8] [11].

A third generation turbine was then design within CMERG. The turbine was created using a similar rotor setup to the previous model scale HATTs. Similarly, the turbine was direct-drive and controlled via a PMSM mounted within the turbine nacelle. In this case a Bosch Rexroth PMSM and drive section was used affording both speed and torque control of the turbine. The turbine was fitted with a thrust and twisting moment transducer for a single blade, as well as an accelerometer housed in the nose cone. The rotor data captured was logged remotely via an Arduino mounted in the turbine nose cone. A similar stanchion arrangement was used to measure thrust loading on the turbine. The torque developed via the turbine rotor was measured via the integrated PMSM. This generation HATT was used for a variety of test campaigns studying turbine rotor faults, the effect of turbine yaw angle, wave loading effects and bend-twist coupling for blade load shedding [12] [13] [14] [15].

In [16] Bahaj et al outline the design and testing of a similar lab scale turbine for both cavitation tunnel and tow tank testing. The turbine was 800mm in diameter and was instrumented with an inline strain gauge dynamometer, located immediately behind the rotor, for torque and thrust measurement. The dynamometer was wired into a full bridge circuit with two gauges on each bridge arm with the output of the bridge wired through slip rings to conditioning circuitry. The measurement range of the instrumentation allowed for accuracies of 71.3 % for power and 71.1 % for thrust at the expected loading magnitudes. The drive shaft was connected via a pulley and timing belt through the vertical support to a further system of pulleys and finally to a DC generator mounted on a platform above the water surface. The DC generator was connected to three rheostats which, for each flow velocity, were altered to control the speed of the turbine rotor.

Various tests were performed in a cavitation tunnel using five pitch angles ranging from 15o to 30o with tunnel speed of up to 2.0 ms^{-1}. For each test the turbine RPM was increased or decreased until cavitation occurred. As well as cavitation testing, tow testing was also conducted for two tip

immersion depths of 150mm (0.19D) and 440m (0.55D) at speeds between 0.8 and 1.5 ms^{-1}. Yaw angles of 0^o to 30^o were investigated along with the operation of the turbine with the addition of a second dummy rotor.

In [17] Clark et al detail the design of a turbine for tank testing to study the positive effects of utilising a contra rotating turbine design to minimise reaction torque on the turbine support structure and swirl in the turbine wake. The diameter of each rotor was 820 mm and the spacing between each rotor was adjustable from 45mm to 100mm. Opposing torques were achieved by the mechanical action of applying a hydraulically actuated disk brake. In order to maintain zero net torque on the drive shaft the braking load was applied to both rotors. Consequently a differential gearbox was designed in order to allow the blades to rotate at different speeds. The turbine was instrumented with optical encoders placed on each of the drive shafts above the water level. Strain gauges were used to measure the thrust on the support, the braking force and therefore the frictional torque as well as the in-plane and normal bending moment on a single blade on each rotor.

Walker et al [18] produced a model turbine to study the effects of blade roughness and bio-fouling on the TST energy extraction process. The turbine used was a two-bladed 0.8 m diameter model, based on the NREL turbine design. The blade profile adopted was the NACA 63-618. The test was conducted in a towing tank with the velocity of the tow carriage set to 1.68 ms^{-1}. The dimensions of the tank were 116 m in length, 7.9 m in width and 4.9 m in depth. The turbine was connected directly to a dynamometer and then through a 90^o gearbox to a differential electromagnetic brake system for turbine speed control. The dynamometer was used to measure the thrust and torque generated by the turbine rotor. The rotational velocity and displacement of the turbine was measured via an encoder. The sample rate for the data acquisition was set at 700 Hz from each of the various sources. The measurement uncertainty was estimated via Taylor series techniques and a confidence figure of 95 % was given. Also a process of removing offset bias was built into the system whereby measurements from each of the sources are taken prior to a testing period, then averaged and the DC bias is removed.

For experimental investigations into turbine mean wake characteristics in shallow turbulent flows [19] produced a 0.27 m diameter model turbine. The testing was undertaken in a channel of 5 m width and 0.45 m depth. A 3 bladed rotor was used to drive a 90^o bevel gearbox which was coupled, via a 4 mm diameter drive shaft, to a motor, mounted above the water level, used to control the turbine velocity. The blade profile used was the Gttingen 804. Thrust on the turbine was measured via strain gauges connected in a full bridge configuration mounted on the rotor support shaft. The effect of turbulence intensity on TST performance was studied by Mycek et al via a three bladed HATT of 0.7 m diameter [20] [21] [22]. The rotor was connected to a speed control motor through a gearbox and used NACA 63418 profile blades. A six component load cell was used to measure the thrust and moment on the turbine, the instrumentation was rated for 1500 N and 1500 Nm and was sampled at 100 Hz. A torque sensor was mounted behind the motor and was sampled at 100 Hz. Flow measurements were made with a laser Doppler velocimeter (LDV).

More recently, Edinburgh University, developed a direct-drive 1/20th Scale model TST of 1.2 m diameter. The turbine boast direct rotor torque and thrust measurements as well as flapwise bending moments on each turbine blade [23].

III. Turbine Design

The previous section outlines considerations and HATT design solutions developed thus far as part of tidal energy research activities. This section details the design of a 3-bladed 1/20th scale HATT based on the experience gathered both during previous turbine development stages and accumulated via the review presented. Initially, the design requirements of the newly developed turbine are presented, followed by an overview of the turbine design. The section then contains a discussion of the design and implementations of differing aspects of the final turbine design.

A. Design Criteria

The turbine design development was undertaken with the research activities proposed as part of the DyLoTTA project in mind and aimed to build on the design and control of previous turbines built within CMERG. The PMSM and drive setup utilised in the last turbine developed allowed for a high degree of fidelity in turbine control, offering stable speed and torque control in a variety of turbine operating conditions.

A list of requirements were drafted and can be seen in Table I. The power production and rated loads were developed with considerations of the non-dimensional thrust and power curves for the previous rotor used within CMERG, which also housed three blades - the blades utilised a Wortman FX63-137 profile. These non-dimensional curves were used as they have been subject to a variety of modelling and validation exercises over the last 7 year of research undertaken at CMERG, offering a high degree of certainty in the peak values used for design calculations [7] [9] [13]. A safety factor of 1.5 was used to ensure that, with the redeveloped blade design, the newly created turbine would withstand the loadings experienced. The rated mean fluid velocity for the turbine was set at 1.3 ms^{-1} with turbulence intensities of up to 15 %, leading to a maximum instantaneous fluid velocity of up to 1.5 ms^{-1}.

The design loads for the turbine were developed using the standard equations for power, torque and thrust loading for a HATT, along with the appropriate non-dimensional values as discussed above. The equations are given as:

$$Power = \frac{1}{2} C_p(\lambda) \rho A V^3 \tag{1}$$

$$Torque = \frac{1}{2} C_\theta(\lambda) \rho A R V^2 \tag{2}$$

$$Thrust = \frac{1}{2} C_t(\lambda) \rho A V^2 \tag{3}$$

where,

$$\lambda = \frac{\omega R}{V} \tag{4}$$

TABLE I
TABLE OUTLINING THE MAIN DESIGN SPECIFICATIONS AND INSTRUMENTATION LIST FOR THE DEVELOPED HATT.

Requirements List	
Specification	Details
Rated Flow Velocity	Continuous: 1.3 ms^{-1}, Instantaneous: 1.5 ms^{-1}
Rated Power	0.6 kW
Maximum Rotational Velocity	350 RPM
Rated Torque	Continuous: 41 Nm, Instantaneous: 54 Nm
Maximum Rotor Thrust	1.07 kN
Maximum Blade Root Bending Moment	Flapwise: 129.76 Nm, Edgewise: 18.13 Nm
Control Types	Speed Control, Torque Control, Regulated Torque Control, Optimal λ control
Instrumentation List	
Flap-wise and Edge-wise blade root bending moments (each blade); Rotor Thrust; Rotor Torque; Rotor Position; Rotational Velocity; PMSM Torque; Stanchion Bending Moment; Support Structure Vibration.	

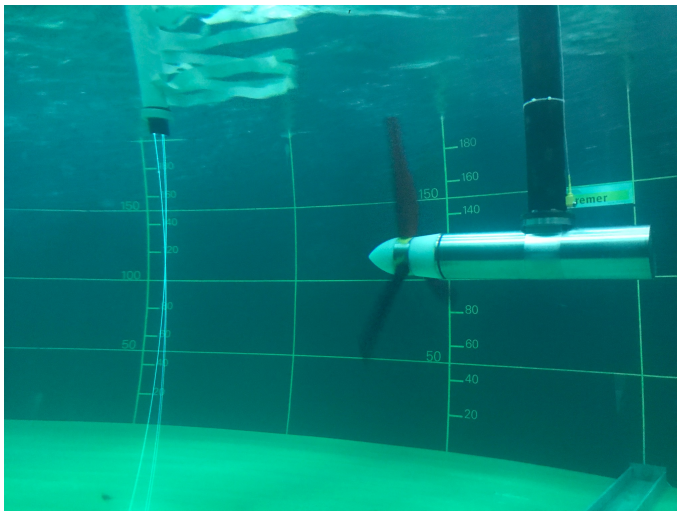

Fig. 1. The developed 1/20th scale HATT in-situ at IFREMER

Where in equations (1) to (4), V is the fluid velocity in ms^{-1}, ρ is the density of water in kg/m^3, A is the turbine swept area in m^2, R is the turbine radius in m and ω is the rotational velocity in $rads^{-1}$.

B. Design Overview

The turbine developed is of 0.9 m diameter, relating approximately to 1:20 scale in comparison to a 20 m diameter HATT. Figure 1 shows the turbine in-situ during testing at the IFREMER flume facility in Boulogne, France, undertaken in April 2018. Figure 2 shows a Solidworks render of a section view through the turbine. The turbine rotor houses 3 blades based on the Wortman FX 63-137 blade profile. The HATT is direct-drive with turbine control and power take-off undertaken by a Permanent Magnet Synchronous Machine (PMSM). The power flow from the turbine and its associated braking torque is controlled by a drive series which make up back-to-back Voltage Source Converters (VSCs) either side of a DC bus.

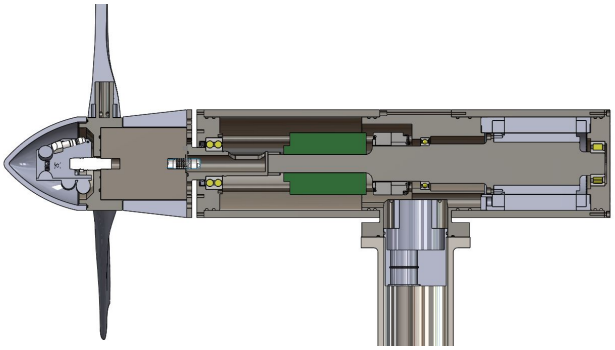

Fig. 2. Soliworks rendering of the 1/20th scale HATT.

The front section of the turbine was developed to house an instrumentation suite consisting of an integrated rotor thrust/torque transducer, an encoder and an instrumented rotor. The instrumented rotor was developed to measure, 'flap-wise' and 'edge-wise' blade root bending moments for each turbine blade.

Additional installed instrumentation includes a moisture sensor, stanchion bending moment measurements and support structure vibration measurements. The instrumentation wiring is transferred into the rotational reference frame by an 18-way slip ring mounted on the turbine drive shaft. The turbine body is flanged together with the support stanchion through which the power, encoder and instrumentation cables are fed.

At the time of writing, the design outlined has been used to create a single turbine. However, as part of on going research activities a further two turbines are currently in production. The further two turbines are being developed to the same specification detailed below. The ultimate goal is to have the ability to test the three turbines in a number of array configurations, under various wave conditions and with differing turbulence characteristics in the on-coming flow.

C. Blade Design

Figure 3 shows an example of the newly developed blade.The original blade modelled at Cardiff University used the Wortmann FX63-137 aerofoil. It was initially designed as a self-starting turbine and as such had a high twist from root to tip of 35 degrees and a large chord length at the root. By having a large twist at the root the relative flow angle is increased allowing the ability to self-start.

The design of the new blades still uses the Wortmann profile to keep it in line with the previous design, but the ability to self-start was no longer needed. Self starting was no longer required due to the increased ability to control turbine operation via the integration of the PMSM. Variations for the twist were modelled using the Blade Element Momentum Theory (BEMT) code developed at Strathclyde University by Nevaleinen [24]. For each twist distribution four pitch angles were trialled in the aim to give the optimum conditions. The lift and drag coefficients used in the BEMT code were determined using XFoil.

Fig. 3. The adapted Wortman FX 63-157 blade.

Once the design had been optimised using the steady BEMT it was then drawn and modelled using ANSYS CFX. A mesh independence study was conducted, focussed primarily on the moving reference frame (MRF) mesh density and the face sizing on the blades. The turbine was first modelled without the stanchion as the steady BEMT code does not take this into consideration.

There was good comparison between the CFD and BEMT for both the Ct and Cp graphs. The TSR for peak Cp was found to be around 4 with freewheeling occurring near TSR 6.5. The stanchion was added to the model and re run for flow velocities ranging from 0.3 to $1.3ms^{-}1$. The effect of the stanchion resulted in the Cp being around 9% lower because of the increased velocity deficit behind the blades. In running between a large range of flow velocities the Reynolds independence was looked at and independence was found to occur in the region of 0.5 to $0.6ms^{-}1$.

D. Drive Train Design

Figure 4 shows the an overview of the final drive-train design for the 1/20th scale model HATT. As mentioned the turbine was designed with a direct-drive drive-train arrangement. As shown in Figure 4, it was created via two drive interfacing shafts to allow for the flanging arrangement to the torque/thrust transducer. USing two drive shafts also facilitated positioning of the PMSM on back side of the turbine away from the rotor instrumentation.

The drive shaft is supported by three bearing housings, namely, the mid support, front and back plates. The first shaft has a hollowed section to accommodate instrumentation cabling, which is fed from the rotating portion of the 18-way slip ring. The front shaft is supported by back-to-back deep groove ball bearings which have been set-up and selected to act as the main thrust bearing and are housed in the front plate. A dynamic seal was embedded in the front plate to protect from water ingress between the shaft and the front plate.

The main drive shaft is supported in two places, at the mid support and back plate. A deep groove ball bearing supports the shaft at the mid section and roller bearing supports the rear of the shaft, housed in the end plate. A roller bearing was used in this instance to aid with assembly and disassembly. The front and back drive shafts are coupled together using a tongue and groove set up to transfer torsional loads and rotational motion. The main shaft has been fitted with an encoder and slip ring to the left of the mid plate and a PMSM to the right of the mid plate.

E. Permanent Magnet Synchronous Machine, Drives and Control

The model scale HATT houses an embedded PMSM for turbine breaking and control. The PMSM used is a Bosch Rexroth MST 130E. The ratings of the motor are presented in Table II. The motor was chosen for its relative high torque capacity for a non-directly cooled motor as required by the direct-drive configuration. The rotor of the PMSM houses permanent magnets arranged into 10 pole pairs and is mounted on the back drive shaft fastened via a flange. The stator contains the motor windings and is integrated via the mid-section and back plates of the HATT. To cool the motor appropriately the motor is press fitted into the stainless steel back cover of the HATT. Circular steps on the mid-section and back plate align the stator relative to the drive shaft to preserve the air gap of 0.4 mm.

Power flow to and from the PMSM is managed by a drive section, which is located in a cooled drive cabinet either on the tow carriage or on the flume side. Figure 5 shows the drive cabinet. The drive sections are made up of a mains choke, a mains filter, a rectifier and an inverter (or three inverters when operating all three turbines). A three phase connection is made to the mains choke which manages regenerative energy feedback into the grid when required. The three phase connection is the made between the mains choke and the mains filter, filtering is undertaken to maintain power quality in the supply to the rectifier. The filtered three phase connection is then fed to a rectifier where the AC current is converter to DC via a VSC with a switching frequency of 4000 Hz. The rectifier and inverter are connected via a DC bus integrated with a DC bus capacitor. The inverter then creates a three phase AC current which is connected to the motor. The power flow to and from the motor are managed by the VSCs either side of the DC bus - similar to back-to-back set up used for HATTs and wind turbines adopting a direct-drive PMSM topology. The back-to-back VSCs allow for servo based Vector Oriented control

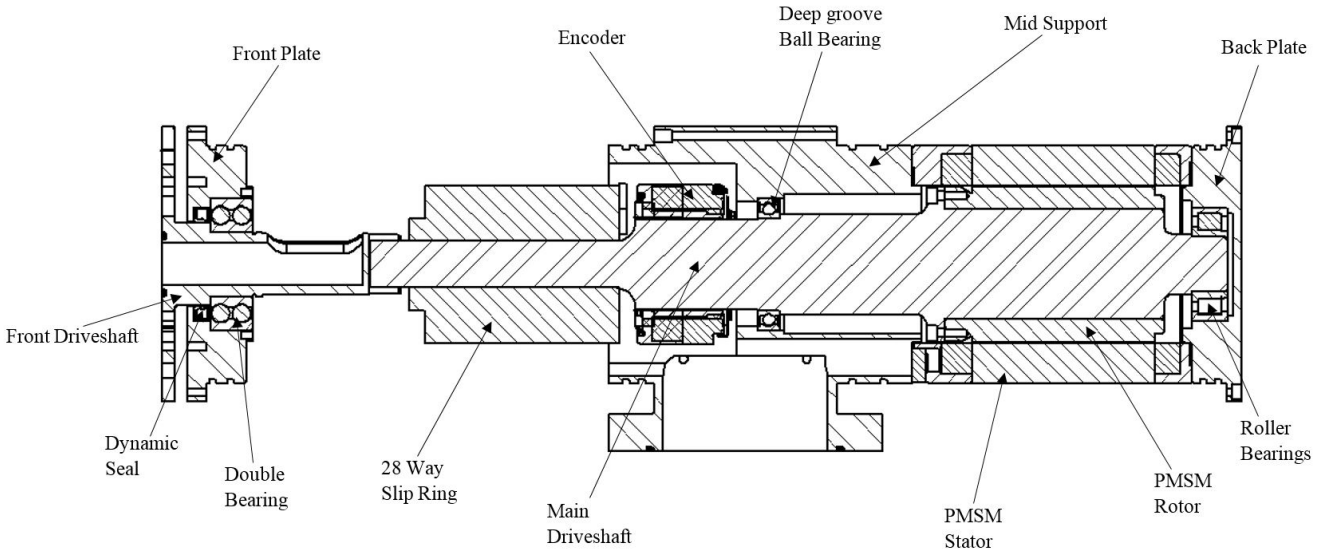

Fig. 4. The developed 1/20th scale HATT in-situ at IFREMER

TABLE II
THE MOTOR PARAMETERS FOR THE BOSCH REXROTH MST130E.

Motor Parameters	
Rated Torque	42 Nm
Maximum Speed	350 RPM
Rated Power	0.6 kW
Maximum Rotational Velocity	350 RPM
No. of Pole Pairs	10
Winding Resistance	14.9 Ω
Mass of Stator	7.7 kg
Mass of Rotor	2.2 kg

of the turbine to directly the torque required of the PMSM or via an additional velocity control loop the desired rotational velocity. The encoder required for servo-control of the PMSM is detailed below.

F. Instrumentation

An instrumentation suite was integrated into the turbine in order to quantify dynamic loadings on the HATT under various on coming fluid flow regimes. Below an overview of the instrumentation suite integrated into the turbine is presented.

1) Rotor Torque and Thrust Transducer: A bespoke rotor torque and thrust transducer was created by Applied measurements. The transducer used was an adapted DBBSS/TSF Torque and Axial Force Sensor, which had a rated maximum thrust load of 1.8 kN and a maximum rated torsional loading of 100 Nm. The transducer was adapted for the specified rating, for waterproofing, to house two 18 way Lemo EGG.2B.318 connectors and to accommodate 'through' wiring for hub instrumentation. The transducer was fastened to the front drive shaft and to the turbine rotor via a flanges on either side. The transducer used two ICA4H amplifiers, one for Thrust loading and one for Torque loading, both of which were housed in the body of the transducer. The Thrust loading amplifier was set to give a sensitivity of 0.005 mA/N and the torque loading amplifier was set to give a sensitivity of 0.08 mA/N. The transducer was mounted up stream of any bearings or seals to measure rotor loads prior to any drive shaft losses.

2) Instrumented Hub: The turbine hub was created to house the blades and measure both flap-wise and edge-wise bending moments on each of the three turbine blades. Figure 6 shows a Solidworks rendering of the hub design. The hub is a circular section with holes for flange fixing to the Thrust/Torque transducer, a hole in the centre accommodates a Lemo connector for instrumentation wiring. Lastly, three 'bosses' project radially from the outside of the circular section, to which the blades are attached via grub screws. The three bosses are spaced at 120^o and each of the bosses houses two full-bridge strain gauge set ups for measuring blade root bending moments.

The bosses have a small step machined into them to allow for grub screw fastening of the turbine blades. Each of the bosses have four, 'flats' machined into them, two parallel to the turbine rotational axis and two perpendicular to the turbine rotational axis. These flats were included accommodate the aforementioned two full-bridge strain gauge set ups for measuring blade root bending moments.

In order to correctly set the diameter of the bosses a bending moment and Finite Element Analysis study was undertaken. The goal of the study was to limit the stress on the machined faces to 30% of the material yield stress and whilst setting a suitable strain level on the faces. The range of suitable diameters was first considered using simple beam bending equations. The following expression was used to find the strain at the blade root for differing outer radii of the bosses:

$$\sigma = \frac{PL}{Z} \tag{5}$$

where,

$$z = \frac{0.78(r_o^4 - r_i^4)}{r_o} \tag{6}$$

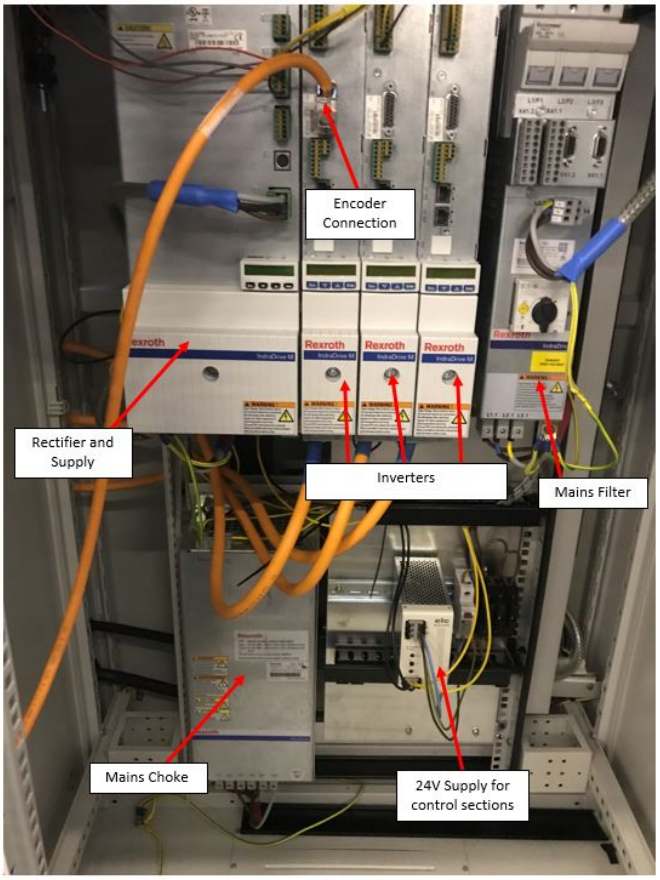

Fig. 5. The drive cabinet used for turbine control and power management.

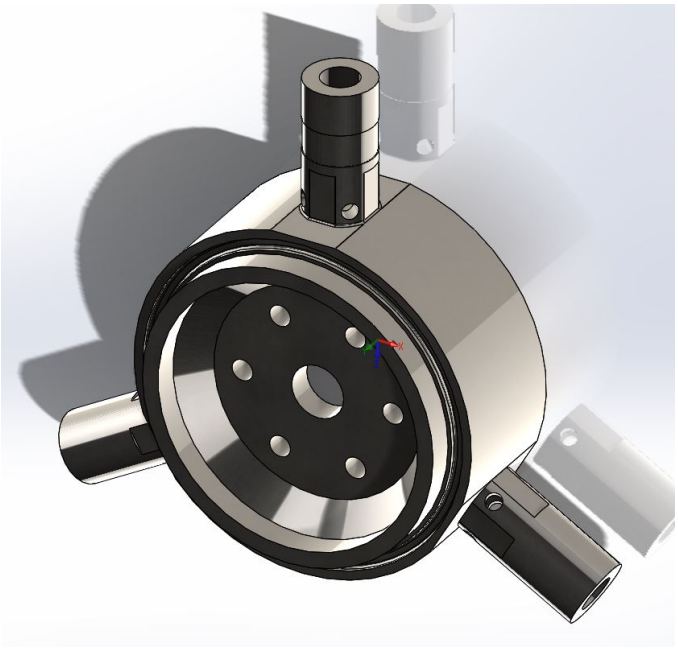

Fig. 6. Solidworks rendering of the instrumented hub.

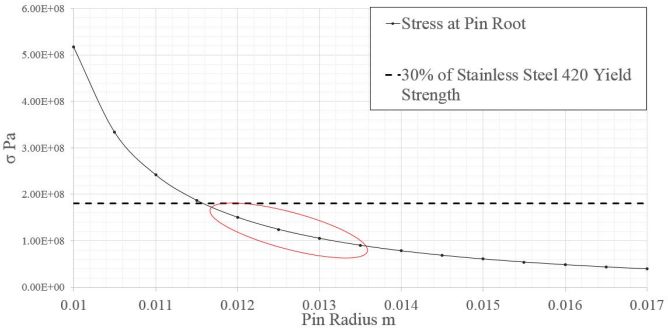

Fig. 7. Figure showing the stress at the blade root resultant from the maximum expected thrust loading on a blade - applied at 75% of the blade length.

here, P refers to the load applied to the blade in Newtons at a distance L from the blade root, r_o refers to the inner radius of the boss and r_o the outer radius of the boss, where all lengths have the units meters.

Figure 7 shows the results of the calculations performed. As no non-dimensional blade root bending moment curves had been developed for the rotor, the calculation was undertaken by setting the applied load to 1/2 the maximum thrust load expected at the turbine rotor - that is, 1/3 of the total rotor thrust loading with a safety factor of 1.5 applied. For the calculation, the load was considered to have been applied at 0.75 of the blade length which is approximately the centre of pressure for the blades at free wheeling.

It can be seen in Figure 7 that the required outer radius of the bosses was between 12 mm and 13.5 mm. As such, the boss diameter was set to 26 mm with the distance between the flats set to 24mm. An FEA study was then under taken to confirm that no excessive loadings would occur given the boss set up defined via the process outlined above. It was found that the FEA gave a maximum strain on the boss root of 22.69 % of the material yield stress which was comparable to 22.06 % found in the beam bending calculation outlined above. The average strain in the principle direction on the flats was found to be 353 μstrain. The resulting arrangement gave the following sensitivities for blade rate bending moment measurements: Flapwise Bending Moment: 1.39 mV/V and Edgewise Bending Moment: 0.62 mV/V.

3) Encoder: Figure 4 shows the position of the hollow through shaft rotary encoder used for position feedback as required for servo control of the PMSM. The encoder selected was and optical encoder, the model utilised was the Heidenhain ENC113 encoder with Endat 2.2 interfacing. The encoder is of 13 bit type with a quoted system accuracy of $\pm$ 20 seconds of arc.

4) Stanchion Instrumentation: The stanchion instrumentation varies and is based on the test campaign being undertaken. To-date, two sets of instrumentation have been utilised. Firstly, strain gauges in a full-bridge configuration were applied to the stanchion to measure induced bending moments on the turbine support structure. The gauges were oriented to measure the Thrust-wise bending moment on the support structure with all gauges oriented to measure the principle strain direction. The

gauges were applied as closely as practicable to the stanchion clamping arrangement. The bridge signal was amplified by an SGA strain gauge amplifier, where the gain was set via consideration of the voltage reading at the maximum expected load.

Additionally, two industrial accelerometers have been integrated into the support structure. The goal of this additional instrumentation is to measure vibration propagation through the support structure. The accelerometers used were of the Monitran Vibration Sensor MTN/1830SM8.

5) Amplification and Signal Processing: The blade load and thrust/torque transducer measurements all utilised integrated circuit ICA4H amplifiers. The output of the amplifiers is between 4 mA and 20 mA and can accommodate bridge systems with sensitivities between 0.5 mV/V and 150 mV/V. A gain setting resistor is used to achieve measurements in the 4 mA to 20 mA range for differing bridge sensitivities. The amplifier required 24 V input and outputs a regulated 5 V supply to the wheatstone bridge configurations. The amplifier has an inbuilt low-pass filter with a fixed cut-off frequency of 1 kHz.

The stanchion bending moment instrumentation, consisting of a full-bridge configuration of strain gauges, is amplified and filtered by a PCM Strain Gauge Amplifier(SGA). The PCM SGA is set to filter the amplifier output at 1 kHz. Lastly, the piezo-electric vibration sensors signals are not amplified and are filtered at the NI9234 DAQ card by a low pass filter with the cut-off frequency set to set to 5kHz. The low pass filters cut-off values are set to act as an anti-aliasing filter to ensure quality of transient analysis of the captured loading and vibration data. Table III shows the sample rate and anti-aliasing filter cut-off frequency for each piece of instrumentation.

6) Data Acquisition: Data acquisition for all three turbines is undertaken via a National Instruments Compact RIO. The DAQ cards used in the compact RIO are outlined in Table III. The table shows the measurement type, bit depth, sample rate and anti-aliasing filter cut-off frequency for each of the channels. A Compact RIO was utilised due to the advantages of being able to utilise both the Field Programmable Gate Array (FPGA) and the Real-Time operating system for test control and data capture and management. The tasks undertaken by the Compact RIO have been broadly split into data capture and triggering, which is undertaken by the FPGA and data management and test control which is undertaken by the Real-Time operating system.

7) Waterproofing and Moisture Sensor: Figure 8 shows an overview of the sealing arrangement for the main turbine assembly. Generally, sealing of the turbine was accomplished using O-rings, with O-ring sizing and groove specification undertaken following the BSI 4518 British standard. As mentioned a dynamic seal was utilised to seal around the entry point of the front drive shaft into the turbine nacelle through the front plate.

An interlock moisture sensor was integrated into the turbine to alert the user in the event that any of the outlined sealing arrangements failed and water ingress into the turbine occurred. This feature was required for both safety and to protect the scale model HATT hardware. The circuit was connected to 10 V source, output from the Compact RIO; in the event of water ingress the two moisture probes are shorted or connected together. The shorting of the two probes changes the circuit output from 10 V to 0V (ground). A 0 V reading from the moisture sensor then starts an automatic shut down of the turbine PMSM to avoid any electrical damage. Lastly, the user is alerted of the leak so the turbine can be removed from the tow tank or flume.

TABLE III
TABLE OUTLINING THE NI DAQ CARDS USED FOR DATA CAPTURE ALONG WITH INFORMATION ON THE MEASUREMENT TYPE, BIT DEPTH, SAMPLE RATE AND ANTI-ALIASING FILTER CUT-OFF FREQUENCY.

Measurement Type	DAQ Card	Bit Depth	Sample Rate	Anti Aliasing Cut-off
Blade root bending moment	NI9203	16-Bit, 0-20 mA	2 kHz	1 kHz
Rotor Thrust	NI9203	16-Bit, 0-20 mA	2 kHz	1 kHz
Rotor Torque	NI9203	16-Bit, 0-20 mA	2 kHz	1 kHz
Stanchion Bending Moment	NI9207	24-Bit, 0-10 V	2 kHz	1 kHz
Stanchion Vibration	NI9234	24-Bit, 0-100 mV	10 kHz	5 kHz

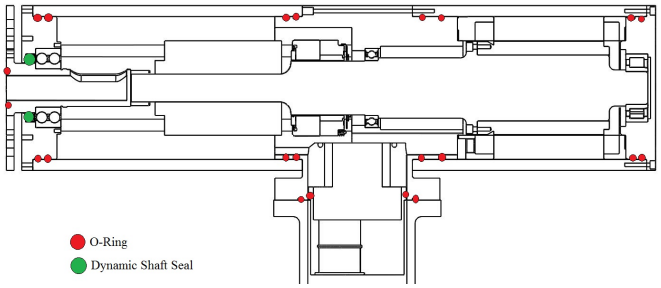

Fig. 8. Overview of the sealing arrangements for the 1/20th Scale HATT.

IV. Initial Testing and Turbine Characterisation

Since the development of the detailed model scale HATT, a number of testing campaigns have been undertaken to commission the HATT, allowing for instrumentation and control checks. Furthermore, the test campaigns allowed initial characterisations of the developed model scale HATT under both speed and torque control operation. Below, details of testing in the wave tow tank at the INSEAN facility, Rome are presented. This testing was facilitated by MaRINET 2 and allowed commissioning and testing of the HATT under various control schemes and wave conditions.

A. INSEAN Testing

Following the method of [25] tests were conducted by attaching the scaled model HATT to the carriage and towing

Fig. 9. Test set-up in the INSEAN wave-tow facility a) horizontal axis turbine mounted on the tow carriage via stanchion b) measurement equipment set-up, 1: wave probe bank with circled ultrasonic probe used in this analysis, 2: electromagnetic current meter, 3: Pitot tube

it along the tank. Figure 9 shows the turbine installed on the carriage. A 0.09 m diameter stanchion held the turbine rigidly in place, attached by two sets of brackets to the tow carriage. The turbine hub centre was set 1.5 m below the still water surface, and centred in the cross-stream direction. Cables from the turbine were run along the inside of the stanchion and connected to the control and data acquisition systems situated on the carriage. Additional measurement systems were employed to monitor the flow conditions during testing: a Pitot tube and an electromagnetic current meter were mounted on the side of the turbine at cross-stream distances of 1 m and 1.5 m from the turbine hub centre, as shown in Figure 9.

B. Overview of Characterisation Results

To define the rotor characteristics for the newly developed HATT, non-dimensional Power, Thrust and Torque curves were developed using the data captured as outlined above. The non-dimensional coefficients were calculated by re-arranging equations (1) to (3), using measured data for Power, Thrust and Torque. The fluid velocity, V, was set to the velocity of the tow carriage. The data presented relates to a carriage velocity of 1 ms^{-1}. The non-dimensional values are plotted against tip-speed ratio, λ, as defined in (4). The carriage velocity was used as V and measured rotational velocity as ω. Figures 10 to 12 show the developed non-dimensional curves for the turbine rotor.

Figures 10 to 12 have been plotted with error bars, highlighting twice the standard deviation of the data, to give an indication of the uncertainty associated with the characterisation. Similar non-dimensional characteristics were found for both speed and torque control cases. Repeat tests were also in good agreement, suggesting high repeatability from the set up. Peak power,thrust and torque coefficients of 0.42, 0.84 and 0.145 were found, respectively. Peak power occurred between λ values of 3.5 and 4.5; peak thrust was found at $\lambda = 5.5$ and peak torque was found close to $\lambda = 2.5$. However, further testing is required to refine the quoted values.

V. Conclusions

- The paper presents the design of a 1/20th scale HATT.

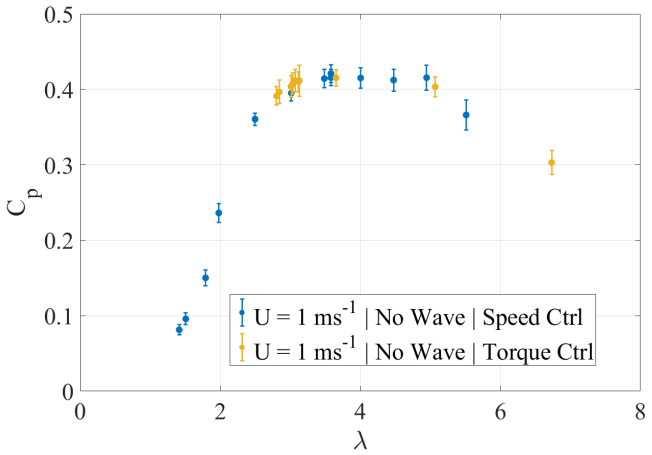

Fig. 10. C_p vs λ curve, for $V = 1ms{-}1$.

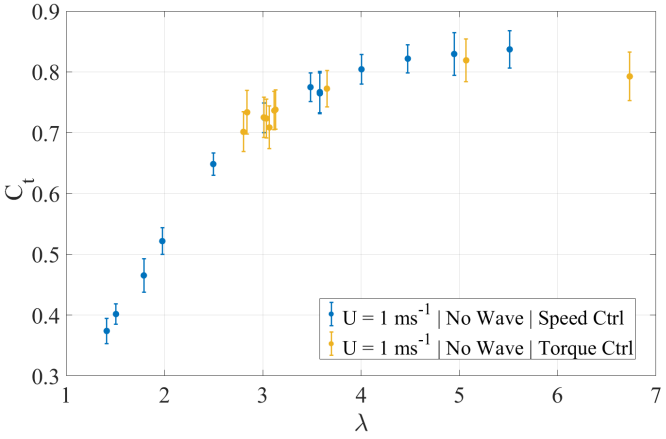

Fig. 11. C_t vs λ curve, for $V = 1ms{-}1$.

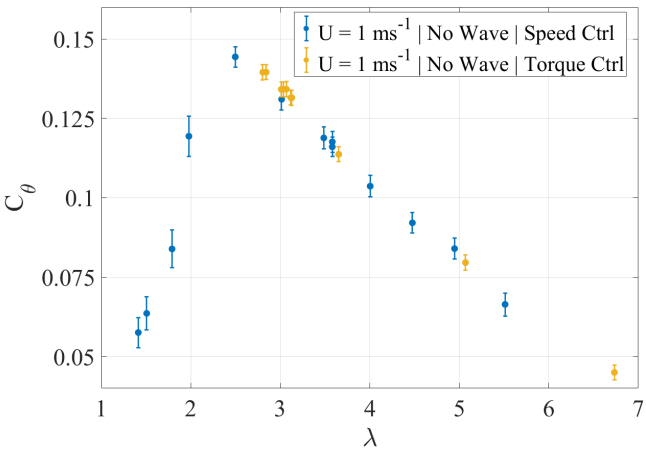

Fig. 12. C_θ vs λ curve, for $V = 1ms{-}1$.

- The turbine instrumentation and design procedure are outlined in brief.
- The commissioning and initial testing of the turbine at the wave tow tank in INSEAN, Rome was discussed.
- A suitable experimental set up was achieved and high repeatability in results was found.
- The characteristics curves for the newly developed turbine are presented - although further testing is required to fully define the turbine operating characteristics.

VI. Further Work

- The design presented is currently being used in the production of a further two turbines.
- The initial turbine developed will be more fully characterised and used to study turbine loading under turbulent flows and a variety of wave scenarios.
- Upon completion, commissioning and characterisation of the further two model scale HATTs, testing will be undertaken to aid understanding of combined wave and array loading effects.

Acknowledgements

The authors would like to thank industrial collaborators Bosch Rexroth and National Instruments. The testing at INSEAN was gratefully funded by MaRINET 2. The DyLoTTA project is EPSRC funded:.

References

[1] Department of Energy & Climate Change, "DECC Electricity Generation Costs 2013 - GOV.UK," Department of Energy & Climate Change, London, Tech. Rep., 2013. [Online]. Available: https://www.gov.uk/government/publications/decc-electricity-generation-costs-2013

[2] X.-P. Zhang and P. Zeng, "Marine Energy Technology [Scanning the Issue]," *Proceedings of the IEEE*, vol. 101, no. 4, pp. 862–865, apr 2013.

[3] C. Johnstone, D. Pratt, J. Clarke, and A. Grant, "A techno-economic analysis of tidal energy technology," *Renewable Energy*, vol. 49, pp. 101–106, jan 2013.

[4] IEC, "IEC 61400 - Wind turbines," IEC, Tech. Rep., 2015. [Online]. Available: https://webstore.iec.ch/publication/22259

[5] M. Lewis, S. Neill, M. Hashemi, and M. Reza, "Realistic wave conditions and their influence on quantifying the tidal stream energy resource," *Applied Energy*, vol. 136, pp. 495–508, dec 2014.

[6] T. Burton, *Wind energy handbook*. Wiley, 2011.

[7] A. Mason-Jones, "Performance assessment of a Horizontal Axis Tidal Turbine in a high velocity shear environment." Ph.D. dissertation, Cardiff University, 2010.

[8] A. Mason-Jones, D. O'Doherty, C. Morris, T. O'Doherty, C. Byrne, P. Prickett, R. Grosvenor, I. Owen, S. Tedds, and R. Poole, "Non-dimensional scaling of tidal stream turbines," *Energy*, vol. 44, no. 1, pp. 820–829, aug 2012.

[9] C. Morris, "Influence of solidity on the performance, swirl characteristics, wake recovery and blade deflection of a horizontal axis tidal turbine," Ph.D. dissertation, Cardiff University, 2014.

[10] S. C. Tedds, R. J. Poole, I. Owen, G. Najafian, S. P. Bode, A. Mason-Jones, C. Morris, T. O'Doherty, and D. M. O'Doherty, "Experimental investigation of horizontal axis tidal stream turbines," in *9th European wave and tidal energy conference (EWTEC). Southampton, UK*, 2011, p. 13.

[11] T. A. de Jesus Henriques, A. Botsari, S. C. Tedds, R. J. Poole, H. Najafian, C. J. Sutcliffe, and I. Owen, "The Effects of Wave-Current Interactions on the Performance of Horizontal Axis Tidal-Stream Turbines," in *2 nd Oxford Tidal Energy Workshop*, 2013, p. 37.

[12] M. J. Allmark, "Condition monitoring and fault diagnosis of tidal stream turbines subjected to rotor imbalance faults," Ph.D. dissertation, Cardiff University, 2016.

[13] M. Allmark, R. Grosvenor, and P. Prickett, "An approach to the characterisation of the performance of a tidal stream turbine," *Renewable Energy*, vol. 111, pp. 849–860, oct 2017.

[14] C. Frost, C. E. Morris, A. Mason-Jones, D. M. O'Doherty, and T. O'Doherty, "The effect of tidal flow directionality on tidal turbine performance characteristics," *Renewable Energy*, vol. 78, pp. 609–620, jun 2015.

[15] S. Ordonez Sanchez, K. Porter, C. Frost, M. Allmark, C. Johnstone, and T. O'Doherty, "Effects of extreme wave-current interactions on the performance of tidal stream turbines," in *AWTEC*, Marina Bay Sands, aug 2016.

[16] A. Bahaj, A. Molland, J. Chaplin, and W. Batten, "Power and thrust measurements of marine current turbines under various hydrodynamic flow conditions in a cavitation tunnel and a towing tank," *Renewable Energy*, vol. 32, no. 3, pp. 407–426, mar 2007.

[17] J. A. Clarke, G. Connor, A. D. Grant, and C. M. Johnstone, "Design and testing of a contra-rotating tidal current turbine," *Proceedings of the Institution of Mechanical Engineers, Part A: Journal of Power and Energy*, vol. 221, no. 2, pp. 171–179, mar 2007.

[18] J. M. Walker, K. A. Flack, E. E. Lust, M. P. Schultz, and L. Luznik, "Experimental and numerical studies of blade roughness and fouling on marine current turbine performance," *Renewable Energy*, vol. 66, pp. 257–267, jun 2014.

[19] T. Stallard, R. Collings, T. Feng, and J. Whelan, "Interactions between tidal turbine wakes: experimental study of a group of three-bladed rotors," *Philosophical Transactions of the Royal Society A: Mathematical, Physical and Engineering Sciences*, vol. 371, no. 1985, pp. 20 120 159–20 120 159, jan 2013.

[20] P. Mycek, B. Gaurier, G. Germain, G. Pinon, and E. Rivoalen, "Numerical and experimental study of the interaction between two marine current turbines," *International Journal of Marine Energy*, vol. 1, pp. 70–83, apr 2013.

[21] ——, "Experimental study of the turbulence intensity effects on marine current turbines behaviour. Part II: Two interacting turbines," *Renewable Energy*, vol. 68, pp. 876–892, aug 2014.

[22] ——, "Experimental study of the turbulence intensity effects on marine current turbines behaviour. Part I: One single turbine," *Renewable Energy*, vol. 66, pp. 729–746, jun 2014.

[23] G. S. Payne, T. Stallard, and R. Martinez, "Design and manufacture of a bed supported tidal turbine model for blade and shaft load measurement in turbulent flow and waves," *Renewable Energy*, vol. 107, pp. 312–326, jul 2017.

[24] T. Nevalainen, C. Johnstone, and A. Grant, "A sensitivity analysis on tidal stream turbine loads caused by operational, geometric design and inflow parameters," *International Journal of Marine Energy*, vol. 16, pp. 51–64, dec 2016.

[25] N. Barltrop, K. S. Varyani, A. Grant, D. Clelland, and X. P. Pham, "Investigation into wavecurrent interactions in marine current turbines," *Proceedings of the Institution of Mechanical Engineers, Part A: Journal of Power and Energy*, vol. 221, no. 2, pp. 233–242, mar 2007.